LncRNA SLC7A11-AS1 promotes the progression of hepatocellular carcinoma by mediating KLF9 ubiquitination

Fan-Lin ZENG[1,2], Jie LIN[3], Xing XIE[2], Yuan-Kang XIE[2], Jian-Hong ZHANG[2], Daofeng XU[2], Xiao HE[2], Feng En LIU[4], Bin-Hui XIE[2,*]

[1]Suzhou Medical College of Soochow University, Suzhou, China; [2]Department of General Surgery (Hepatobiliary and Pancreatic Surgery), The First Affiliated Hospital of Gannan Medical University, Ganzhou, China; [3]Department of Intensive Medicine (Comprehensive Intensive Care Unit), The First Affiliated Hospital of Gannan Medical University, Ganzhou, China; [4]Department of General Surgery (Vascular Surgery), The First Affiliated Hospital of Gannan Medical University, Ganzhou, China

Correspondence: binhuixie333@163.com

Hepatocellular carcinoma (HCC) is a malignant tumor, which seriously threatens the life of patients. LncRNA SLC7A11-AS1 was reported to be abnormally expressed in HCC. Here, the functions and relative molecular regulatory mechanism of SLC7A11-AS1 in HCC were investigated. Nude mice and HCC cells were used as the experimental subjects. Knockdown or overexpression of exogenous genes was conducted in HCC cells. RT-qPCR, IHC, and western blot were employed to evaluate the abundance of genes and proteins. The malignant behaviors were evaluated using CCK-8, clone formation, wound-healing, and Transwell. The locations of SLC7A11-AS1 and KLF9 in cells were determined by FISH and IF assays. The total m6A level was evaluated by dot-blot assay. m6A modification of SLC7A11-AS1 was detected using RNA MeRIP. The interactions among molecules were validated by RIP, ChIP, dual luciferase reporter assay, and co-IP. SLC7A11-AS1 was elevated apparently in HCC cells and HCC tissues from mice. SLC7A11-AS1 silencing could suppress HCC progression, which was validated in *in vivo* and *in vitro* experiments. Furthermore, METTL3 mediated m6A modification of SLC7A11-AS1 to elevate its expression. In addition, SLC7A11-AS1 downregulated KLF9 expression by affecting STUB1-mediated ubiquitination degradation and KLF9 enhanced PHLPP2 expression to inactivate the AKT pathway. Eventually, rescue experiments revealed that KLF9 knockdown abolished SLC7A11-AS1 silencing-mediated suppression of HCC progression *in vivo* and *in vitro*. Our results unveiled that m6A-modified SLC7A11-AS1 promoted HCC progression by regulating the STUB1/KLF9/PHLPP2/AKT axis, indicating that targeting SLC7A11-AS1 might alleviate HCC progression.

Key words: hepatocellular carcinoma; SLC7A11-AS1; STUB1; KLF9; PHLPP2

Liver cancer is one of the most common malignancies worldwide, ranking 7th in morbidity and 2nd in mortality [1]. Hepatocellular carcinoma (HCC) is the main type of liver cancer. The relatively insidious symptoms of HCC lead to difficulties in early diagnosis and frequent intrahepatic and extrahepatic metastasis, which is the main cause of poor prognosis [2]. At present, effective approaches for HCC treatment include surgical resection, liver transplantation, radiofrequency ablation, pharmacotherapy, etc. [3], however, the mortality rate of HCC is still not negligible. Malignant behaviors, such as infinite proliferation, strong capabilities of migration, invasion and metastasis of HCC cells, promote the rapid progression of HCC [4]. Therefore, it is possible to find ways to inhibit HCC progression by exploring the molecular mechanisms that influence the growth and metastasis of HCC cells.

Long non-coding RNAs (lncRNAs) are important components of non-coding RNAs. Massive evidence has determined that a large number of lncRNAs, such as lncRNA-TUG1 and lncRNA AC026401.3, play momentous roles in regulating HCC progression [5–7]. SLC7A11-AS1 was determined to be highly expressed in HCC through transcriptome sequencing [8], suggesting SLC7A11-AS1 might be implicated in HCC progression. Currently, the function and mechanism of SLC7A11-AS1 in HCC have not been reported, which deserves to be investigated. In recent years, growing studies have confirmed that lncRNAs can be modified by N6-methyladenosine (m6A) to participate in regulating pathological process [9]. m6A modification is reversible, mediated by methyltransferase, demethylase, and m6A binding proteins, affecting post-transcriptional gene regulation processes such as RNA splicing, stability, and degradation [10]. However,

whether SLC7A11-AS1 is modified by m6A in HCC has not been explored.

Krüppel-like factor 9 (KLF9), belonging to the KLF transcriptional factor family, has been extensively investigated in tumors. For example, KLF9 was reported to play suppressing roles in multi-tumors including non-small cell lung cancer, ovarian cancer, gastric cancer [11–13]. As expected, KLF9 as a suppressor for HCC has been reported. Sun *et al.* revealed that KLF9 expression was reduced in clinical specimens of HCC and KLF9 suppressed HCC cell growth through increasing p53 stability [14]. It is well known that protein degradation could be achieved by ubiquitin modification [15]. We predicted various ubiquitination enzymes, including STIP1 homology and U-box containing protein 1 (STUB1), could interact with KLF9 through Ubibroswer, suggesting that ubiquitination enzymes, such as STUB1, might mediate KLF9 ubiquitination. STUB1 is an E3 ubiquitin-protein ligase, which mediates the ubiquitination of protein substrates. For instance, SMAD3 and RIPK3 were proved to be substrates for STUB1 [16, 17]. We speculated that STUB1 mediated KLF9 ubiquitination in HCC. Previous studies revealed that STUB1-mediated ubiquitination degradation of protein substrates was regulated by lncRNAs [18, 19]. However, there is no evidence of SLC7A11-AS1 regulating STUB1-mediated ubiquitination degradation.

Pleckstrin homology domain leucine-rich repeat protein phosphatases (PHLPPs), including two members PHLPP1 and PHLPP2, are serine/threonine protein phosphatases, which are implicated in suppressing the malignant behaviors of tumors through dephosphorylation of AKT [20–22]. As previously reported, berberine promoted the expression of PHLPP2, which suppressed Akt phosphorylation to stimulate apoptosis of hepatoma cells [23], suggesting PHLPP2 served as a suppressor in HCC through mediating Akt dephosphorylation. hTFtarget database predicted that KLF9 might be a potential transcription factor for PHLPP2, however, these relationships need to be further explored in HCC.

Based on these evidences, we reasonably hypothesize that SLC7A11-AS1 is modified with m6A to regulate STUB1-mediated KLF9 ubiquitination and KLF9 regulates PHLPP2 expression to affect the AKT pathway, thereby promoting the progression of HCC. Our findings might provide novel potential markers to restrain the progression of HCC.

Materials and methods

Tumor formation in nude mice. Animal experiments were approved by the ethics committee of The First Affiliated Hospital of Gannan Medical University. The BALB/c nude mice (male, 15–20 g, 5–6 weeks old) were purchased from Hunan SJA Laboratory Animal Co., Ltd. MHCC97H cells were infected with lentivirus carrying sh-NC or sh-SLC7A11-AS1, sh-SLC7A11-AS1 combined sh-KLF9, which were subcutaneously injected into nude mice for tumor forma-

tion. The tumor volume was evaluated every five days for 5 consecutive weeks. After 5 weeks, mice were sacrificed and tumor tissues were removed for subsequent experiments. In addition, to evaluate the pulmonary metastatic ability of MHCC97H cells in mice, MHCC97H cells with indicated transfection were injected into nude mice through the tail vein. 6 weeks later, the metastatic ability was evaluated by observing lung tissue and conducting HE staining.

Fluorescence in situ hybridization (FISH). To localize the cellular distribution of SLC7A11-AS1, FISH assay was conducted. Cy5-labeled SLC7A11-AS1 probe was synthesized by Servicebio (China). Referring to previous studies [24, 25], tumor tissues from mice and cell samples were processed in steps. Then, the SLC7A11-AS1 probe was used to incubate the samples. DAPI was used to stain cell nuclei. A fluorescence microscope (OLYMPUS, Japan) was employed to detect fluorescence intensity.

RT-qPCR. Total RNA was acquired from cells and tissues of mice using the TRIzol reagent (Beyotime, China). cDNA synthesis was performed using Script Reverse Transcription Reagent Kit (TaKaRa, China). qPCR process was implemented by SYBR Premix Ex Taq II Kit (TaKaRa). The primer sequences were as follows: SLC7A11-AS1 (F): CCTGGGGGAAAAACAACATGAA; SLC7A11-AS1 (R): CGTGAGGTGCCTCCCTGATA; PHLPP2 (F): CTTACATCTCGTCCTTTGCACT; PHLPP2 (R): GGTCGTTCAGTAGGTTCCAGTC; KLF9 (F): AACAC-GCCTCCGAAAAGAGG; KLF9 (R): TCGTCTGAGC-GGGAGAACTT; GAPDH (F): AGGTCGGAGTCAACG-GATTT; GAPDH (R): TGACGGTGCCATGGAATTTG. $2^{-\Delta\Delta Ct}$ formula and GAPDH as reference gene were used to calculate the relative expression of targeted genes.

Immunohistochemistry (IHC). HCC tissues from mice were fixed using 4% paraformaldehyde and then embedded with paraffin. Then, about 5 μm sections were prepared. After retrieving the antigen, the sections were blocked with 1% BSA. The sections were incubated with antibodies against Ki-67 (ab15580, Abcam, UK), KLF9 (710921, Thermo Fisher Scientific, USA), and PHLPP2 (ab227673, Abcam) overnight at 4 °C. The sections were then incubated with HRP-labeled antibodies for 1 h at room temperature. The sections were counterstained with diaminobenzidine (DAB). Finally, the images were acquired using a Nikon digital camera system (Japan) combined with an Olympus microscope (Japan).

Hematoxylin and eosin (H&E) staining. HCC tissues from mice were cut into 5 μm thick serial sections after fixation with 4% paraformaldehyde solution and embedded with paraffin. Sections were stained with hematoxylin and then stained with eosin (Beyotime). The stained sections were imaged using an optical microscope with a camera (Olympus, Japan).

Cell culture. Hep 3B2.1-7 and MHCC97H cells were obtained from ATCC (USA). Bel-7405 cells were purchased from the Cell Bank of the Type Culture Preservation Committee of the Chinese Academy of Sciences (China).

293T, LO2, Hep 3B2.1-7, HepG2, Huh7, and Bel-7405 cells were obtained from the Cell Bank of Chinese Academy of Sciences (China). All cells were cultured in Dulbecco's modified Eagle's medium (DMEM, Thermo Fisher Scientific) supplemented with 10% FBS (Thermo Fisher Scientific) and 1% antibiotics (Beyotime) under the condition of 5% CO_2 and 37 °C.

Cell transfection. The small interfering RNA targeting METTL3 (si-METTL3), the short hairpin RNA targeting SLC7A11-AS1 (sh-SLC7A11-AS1) or KLF9 (sh-KLF9), overexpression vector of KLF9 (oe-KLF9) or STUB1 (oe-STUB1) as well as their negative control group (si-NC, sh-NC, oe-NC) were obtained from GenePharma (China).

The detailed sequences were as follows: si-METTL3: UCGCUUUACCUCAAUCAACUC, sh-SLC7A11-AS1: AATTGcaaatcataactacatttaagTCAAGAGcttaaatgtagttat-gatttgTTTTTT, sh-KLF9: AATTGctcccatctcaaagcccat-taTCAAGAGtaatgggctttgagatgggagTTTTTT. Huh7 and MHCC97H cells were seeded into 6-well plates and incubated overnight. Then, cells were transfected with the above sequences or plasmids for 48 h using Lipofectamine™ 3000 (Invitrogen, USA) following the instructions.

Cell count kit-8 (CCK-8) assay. Huh7 and MHCC97H cells underwent different transfections and were seeded into 96-well plates and cultured for 24 h, 48 h, 72 h, and 96 h, respectively. CCK-8 solution (10 μl, Beyotime) was added into each well for 2 h incubation. The absorbance was detected by a spectrophotometer (Bio-Rad, Hercules, USA) at 450 nm.

Clone formation assay. Huh7 and MHCC97H cells with different transfections were seeded into 6-well plates and incubated at 37 °C. 2 weeks later, methanol was applied for the fixation of cells and 0.1% crystalized violet (Sigma-Aldrich, USA) was used for staining of cells. The cloned cells were observed and calculated under an optical microscope with a camera (Olympus, Japan).

Wound-healing assay. Huh7 and MHCC97H cells underwent different transfections and were plated on 6-well plates with cellular monolayers overnight. Subsequently, cells were scraped with a micropipette tip. PBS solution washed cells and cells were continually cultured for 48 h. The scratched widths were observed under an optical microscope with a camera and recorded at 0 and 48 h.

Transwell assay. A 24-well Transwell insert system (Corning, USA) was employed to evaluate the invasion ability of Huh7 and MHCC97H cells. The top Transwell chamber was covered with Matrigel (Becton Dickinson Biosciences, USA). Huh7 and MHCC97H cells were seeded onto the upper chamber containing serum-free DMEM and the lower chamber was added with DMEM and 10% FBS. After 24 h, the invaded cells on the below side of the chamber were fixed with 95% alcohol. 1% crystal violet (Sigma-Aldrich, USA) staining was performed to stain the invaded cells. An optical microscope with a camera was employed to observe invaded cells.

RNA m6A dot-blot assay. Total RNA was denatured at 65 °C for 5 min. Then, the samples were spotted onto an NT membrane. After cross-linking with UV and blocking with 5% skim milk, NT membranes were incubated with m6A antibody (ab208577, Abcam) overnight at 4 °C. HRP-labeled secondary antibody was added to the NT membrane for 1 h at room temperature. The membrane incubated with ECL chemiluminescent reagent (Beyotime) was visualized using the chemiluminescence imaging analysis system (Tanon, China).

m6A immunoprecipitation (MeRIP). Total RNA was isolated from Huh7 and MHCC97H cells using TRIzol regent. Anti-m6A (ab208577, Abcam) or anti-IgG (ab172730, Abcam) conjugated with A/G magnetic beads were applied for incubating RNA samples. Subsequently, RNA was precip-itated by beads and then eluted. The precipitated RNA was detected by qRT-PCR after elution and purification.

RNA immunoprecipitation (RIP) assay. Huh7 and MHCC97H cells were lysed with RIP lysis buffer. The super-natants were obtained after centrifugation. The magnetic beads conjugated with antibodies anti-METTL3 (ab195352, Abcam), anti-KLF9 (ab227920, Abcam), anti-STUB1 (ab134064, Abcam), or IgG (ab172730, Abcam) were added into the supernatants. IgG acted as a control. The beads-bound complexes of RNA were eluted with elution buffer. Then, immune-precipitated RNAs were determined using qRT-PCR.

Western blot. The total protein was extracted from Huh7 and MHCC97H cells using RIPA buffer (Beyotime). After quantification of the protein concentration using a BCA protein kit (Beyotime), the proteins were separated by SDS-PAGE and then were transferred onto the PVDF membrane. After blocking with 5% BSA for 1 h, the PVDF membrane was incubated with primary antibodies including METTL3 (ab195352, 1:1000, Abcam), KLF9 (NBP2-45511, 1:1000, Novus, USA), PHLPP2 (ab227673, 1:400, Abcam), AKT (10176-2-AP, 1:5000, Proteintech, China), p-AKT (28731-1-AP, 1:3000, Proteintech), Ubiquitin (ab134953, 1:5000, Abcam), and GAPDH (ab8245, 1:5000, Abcam) overnight at 4 °C. Subsequently, the HRP-conju-gated secondary antibody was applied to incubate the PVDF membrane for 1 h. ECL chemiluminescent reagent (Beyotime) and Odyssey Clx Imaging System (Licor Biosci-ences, USA) were employed to detect protein bands. The densitometry analysis was estimated by ImageJ.

Immunofluorescence (IF). Huh7 and MHCC97H cells transfected with HA-KLF9 were subjected to fixation using 4% PFA. 0.1% Triton X-100 was applied for permeabili-zation for cells. After blocking with 5% BSA, the primary antibody against HA (ab1424, 1:200, Abcam) was used for cell incubation overnight at 4 °C. After PBST washing of Huh7 and MHCC97H cells three times, Cy5-conjugated secondary antibodies were added, and DAPI stained cell nuclei. The images were pictured using a fluorescence microscope.

Chromatin immunoprecipitation (ChIP) assay. Huh7 and MHCC97H cells were subjected to cross-linking reaction with 1% PFA. Chromatin was sonicated to acquire around 200–800 bp fragments. The fragments were incubated with the primary antibody KLF9 (ab227920, Abcam) or IgG (ab172730, Abcam) at 4 °C overnight. Then, the immunoprecipitated samples were subjected to washing, reversal of cross-linking, and DNA isolation. The immunoprecipitated DNA was analyzed using PCR.

Dual-luciferase reporter assay. The wild-type and mutant PHLPP2 promoter sequences (PHLPP2-WT, PHLPP2-MUT) were cloned into a psiCheck2 vector (Promega, Beijing, China). PHLPP2-WT/PHLPP2-MUT and oe-KLF9 were co-transfected into 293T cells using Lipofectamine 3000 Reagent (Invitrogen). Finally, luciferase activity was tested using the dual-luciferase reporter assay system (Promega, Beijing, China).

Co-immunoprecipitation (Co-IP) assay. Firstly, Huh7 and MHCC97H cells were extracted with Co-IP buffer. The lysates were incubated overnight with the antibodies including IgG (ab172730, Abcam) or KLF9 (ab227920, Abcam) antibodies conjugated to Protein A/G beads (Santa Cruz Biotechnology, USA). Afterward, the proteins pulled down by the magnetic beads were eluted and then detected by western blot.

IF-FISH assay. According to a previous study, we conducted an IF-FISH assay [26]. In brief, Huh7 and MHCC97H cells transfected with HA-KLF9 were fixed with 4% PFA and permeabilized with 0.5% Triton X-100. Then, HA (ab1424, 1:200, Abcam), STUB1 (ab134064, 1:300, Abcam), and fluorescent-tagged secondary antibodies were used to incubate cells. After the antibody incubation, cells were fixed with 4% paraformaldehyde and dehydrated in an ethanol series of 70%, 95%, and 100%. The dehydrated cells were then hybridized with a Cy5-labeled SLC7A11-AS1 probe. Images were acquired with a fluorescence microscope (OLYMPUS, Japan).

Cycloheximide (CHX)-chase assay. To explore whether SLC7A11-AS1 affects the stability of KLF9 protein, 12.5 μg/ml CHX (Selleck Chemicals), an inhibitor of protein synthesis, was added into cells. The protein expression of KLF9 was determined by western blot analysis at 0, 2, 4, and 8 h.

Nucleo-plasmic separation experiment. To detect the distribution of SLC7A11-AS1 and KLF9 and interactions between KLF9 and SLC7A11-AS1/STUB1 in cells, nuclear and cytoplasmic of Huh7 and MHCC97H cells were separated using PARIS™ Kit (Invitrogen, USA). Then, nuclear and cytoplasmic RNAs were reverse-transcribed into cDNAs. The distribution of SLC7A11-AS1 and KLF9 was detected by RT-qPCR and the interactions between KLF9 and SLC7A11-AS1/STUB1 were validated by RIP and Co-IP assay.

Statistical analysis. All data were presented as means ± standard deviation (SD). Using GraphPad Prism 9 analyzed all data. Student's t-test was used to analyze the comparison

of two groups and one-way analysis of variance (ANOVA) was applied to conduct the comparison of three or more groups. A p-value <0.05 was regarded as a statistically significant difference.

Results

SLC7A11-AS1 knockdown restrained cell viability, proliferation, migration, and invasion of HCC. Firstly, SLC7A11-AS1 expression was detected in a normal liver cell line (LO2 cells) and HCC cell lines (Hep 3B2.1-7, HepG2, Huh7, Bel-7405, and MHCC97H cells). The results displayed that the SLC7A11-AS1 expression was elevated in HCC cells to varying degrees relative to LO2 cells, and the elevation was most significant in Huh7 and MHCC97H cells (Figure 1A). Therefore, these two cell lines were chosen for subsequent experiments. FISH assay determined that SLC7A11-AS1 primarily located in the cell cytoplasm of Huh7 and MHCC97H cells (Figure 1B). In addition, the nucleo-plasmic separation experiment confirmed that SLC7A11-AS1 was expressed in both the nucleus and cytoplasm, but mainly in the cytoplasm (Figure 1C). To investigate the functions of SLC7A11-AS1 in HCC cells, SLC7A11-AS1 was knocked down using sh-SLC7A11-AS1 transfection in Huh7 and MHCC97H cells (Figure 1D). SLC7A11-AS1 downregulation apparently suppressed cell viability, number of cell clones, cell migration, and invasion (Figures 1E–1H). In total, SLC7A11-AS1 silencing could impair the cell proliferation, migration, and invasion of HCC cells.

SLC7A11-AS1 knockdown suppressed tumor growth and metastasis of HCC. Here, SLC7A11-AS1 was silenced successfully in MHCC97H cells using sh-SLC7A11-AS1 transfection (Supplementary Figure S1A). To explore the role of SLC7A11-AS1 in HCC, BALB/c nude mice underwent subcutaneous injection with MHCC97H cells, which were stably transfected with sh-SLC7A11-AS1. 5 weeks later, the tumor tissues were isolated. We observed that the tumor size and weight in the sh-SLC7A11-AS1 group were greatly decreased compared to the sh-NC group (Figures 2A-2C). FISH assay revealed SLC7A11-AS1 expression was evidently declined in the sh-SLC7A11-AS1 group and the main location of SLC7A11-AS1 was in the cell cytoplasm (Figure 2D). Meanwhile, the decreased SLC7A11-AS1 expression in the sh-SLC7A11-AS1 group was determined by RT-qPCR (Figure 2E). SLC7A11-AS1 silencing notably suppressed Ki-67 (a marker of proliferation) expression, which was evidenced by IHC (Figure 2F). In addition, the effect of SLC7A11-AS1 on tumor metastasis was investigated. MHCC97H cells with sh-SLC7A11-AS1 stable transfection were injected into nude mice through the tail vein. The results displayed that the number of pulmonary metastatic nodules in the sh-SLC7A11-AS1 group was reduced observably (Figure 2G, 2H). Altogether, SLC7A11-AS1 downregulation effectively inhibited tumor growth and metastasis of HCC.
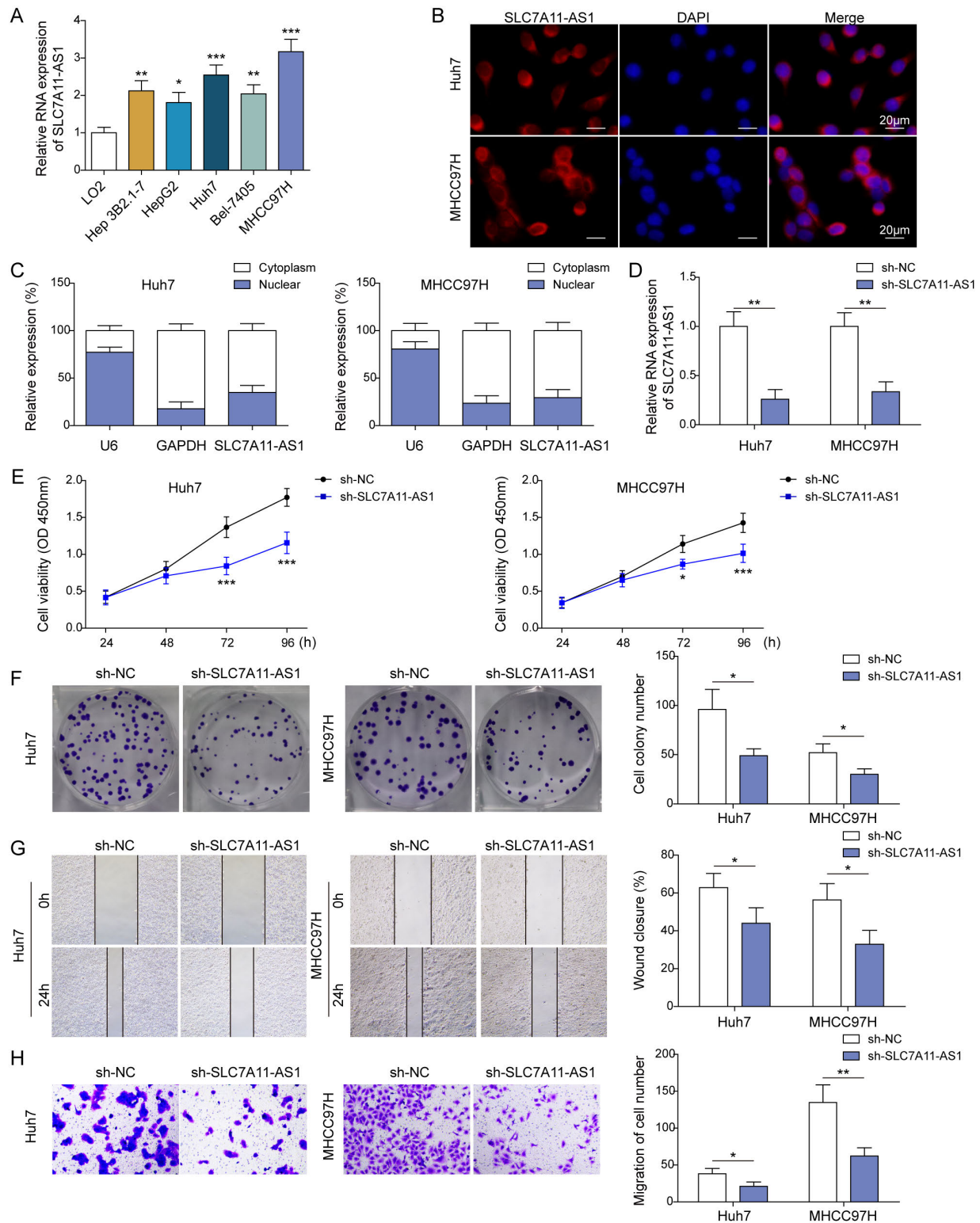
Figure 1. SLC7A11-AS1 knockdown restrained cell viability, proliferation, migration, and invasion of HCC. A) RT-qPCR measured the expression of SLC7A11-AS1 in LO2 cells and HCC cell lines. **B)** FISH assay determined the location of SLC7A11-AS1 in Huh7 and MHCC97H cells. Huh7 and MHCC97H cells were transfected with sh-SLC7A11-AS1 or sh-NC. **C)** The location of SLC7A11-AS1 was detected using a nucleo-plasmic separation experiment. **D)** RT-qPCR measured SLC7A11-AS1 expression. **E)** CCK-8 assay detected cell viability. **F)** Clone formation examined cell proliferation. **G)** Wound-healing tested cell migration. **H)** Transwell determined cell invasion.
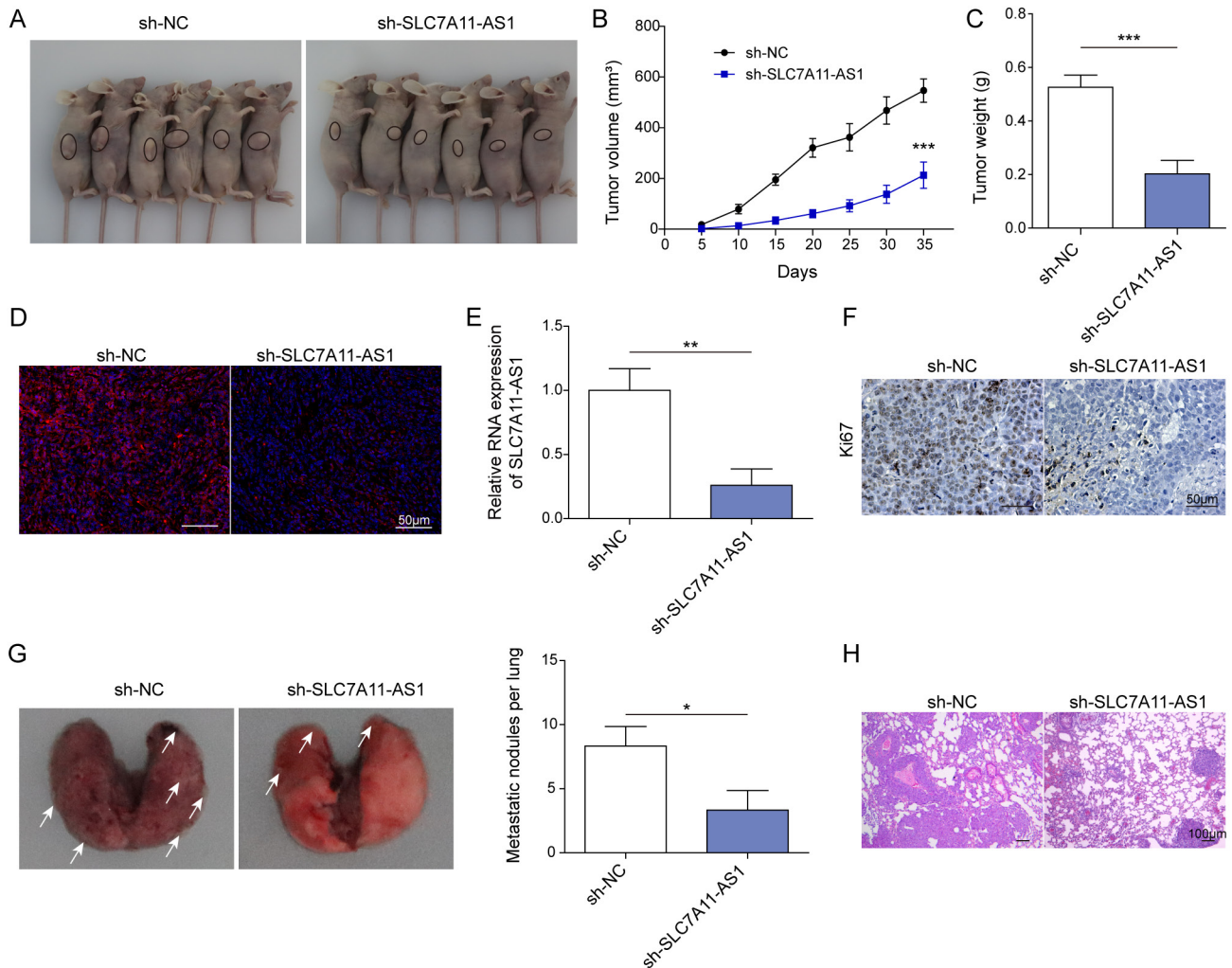
Figure 2. SLC7A11-AS1 knockdown suppressed tumor growth and metastasis of HCC. sh-SLC7A11-AS1-transfected MHCC97H cells were injected subcutaneously into BALB/c nude mice. A) The images of tumors in mice. B) Tumor sizes. C) Tumor weight. D) FISH assay determined the expression and location of SLC7A11-AS1. E) RT-qPCR measured the expression of SLC7A11-AS1. F) IHC detected Ki-67 expression. sh-SLC7A11-AS1-transfected MHCC97H cells were injected into nude mice through the tail vein. G) The images of the lungs of nude mice. H) H&E staining evaluated metastatic pulmonary nodules.

SLC7A11-AS1 was regulated by m6A modification. It was reported that m6A modification of lncRNAs could affect the development of tumors such as HCC [27]. Therefore, we employed SRAMP to predict the m6A site of SLC7A11-AS1 and we found that it had a potential m6A site (Supplementary Figure S2A). Then, m6A dot blot was conducted and higher levels of global m6A were observed in Huh7 and MHCC97H cells compared to LO2 cells (Figure 3A). MeRIP-PCR further determined that the m6A level of SLC7A11-AS1 was elevated in Huh7 and MHCC97H cells compared to that in LO2 cells (Figure 3B). Encouragingly, METTL3 could achieve successful enrichment of SLC7A11-AS1 through the RIP assay (Figure 3C), suggesting an interaction between METTL3 and SLC7A11-AS1. si-METTL3 transfection into Huh7 and MHCC97H cells resulted in decreased METTL3

protein expression (Figure 3D). Furthermore, METTL3 knockdown decreased the m6A level and expression of SLC7A11-AS1 in Huh7 and MHCC97H cells (Figures 3E, 3F). These above results suggested that METTL3 mediated SLC7A11-AS1 m6A modification and enhanced SLC7A11-AS1 expression.

KLF9 activated PHLPP2 transcription to inhibit the AKT pathway. Transcription factor KLF9 was identified as a suppressor of HCC [14]. We were curious to explore the specific molecular regulatory mechanism of KLF9 in HCC. IF assay and nucleo-plasmic separation experiment revealed that the majority of KLF9 was localized in the cell nucleus, but it was also partially expressed in the cytoplasm (Figures 4A, 4B). hTFtarget database predicated KLF9 had potential site on PHLPP2 promoter (Figure 4C). KLF9 could enrich
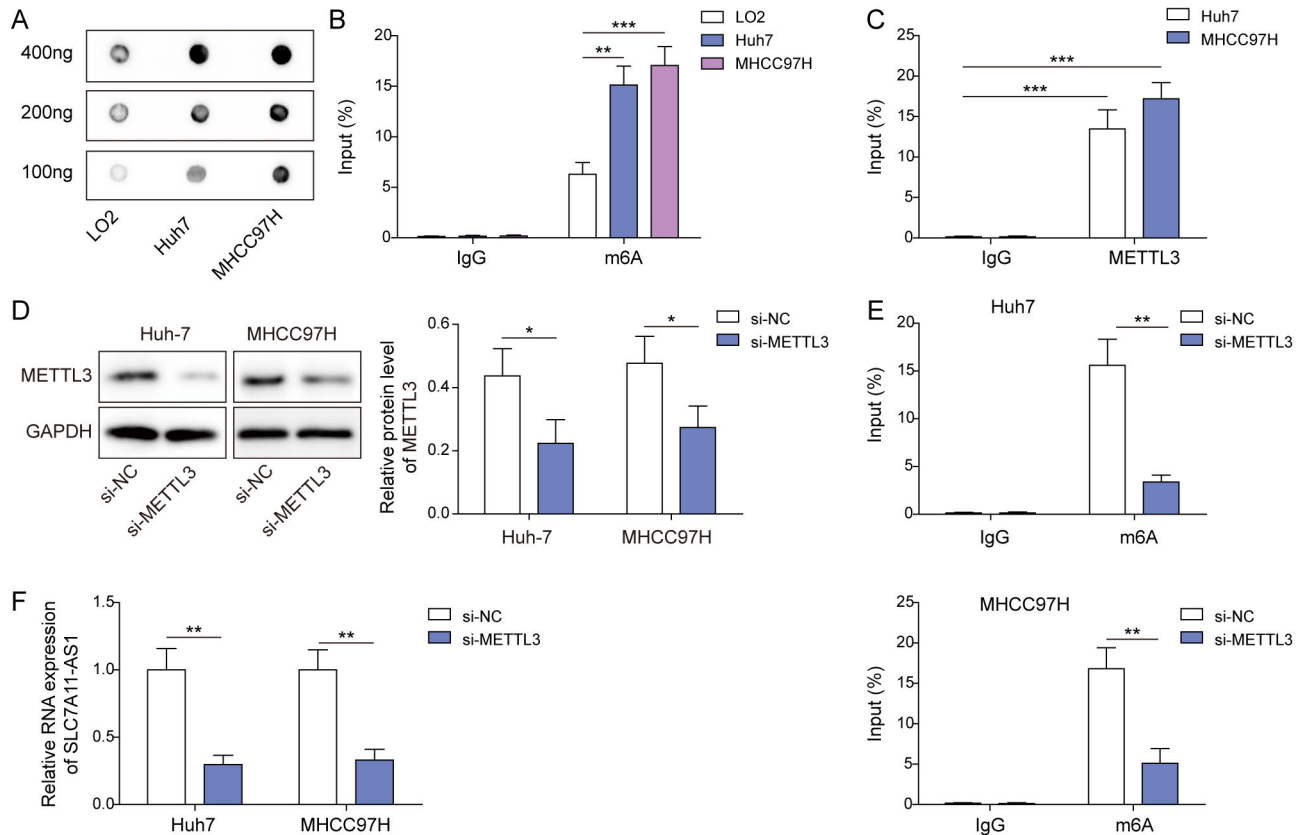
Figure 3. SLC7A11-AS1 was regulated by m6A modification. A) m6A dot blot examined levels of global m6A in LO2, Huh7, and MHCC97H cells. B) MeRIP-PCR determined levels of SLC7A11-AS1 m6A in Huh7 and MHCC97H cells. C) RIP assay validated the interaction between SLC7A11-AS1 and METTL3. D) Western blot detected METTL3 in si-METTL3-transfected Huh7 and MHCC97H cells. E) MeRIP-PCR determined levels of SLC7A11-AS1 m6A in si-METTL3-transfected Huh7 and MHCC97H cells. F) RT-qPCR measured the expression of SLC7A11-AS1 in si-METTL3-transfected Huh7 and MHCC97H cells.

the PHLPP2 promoter evidenced by using ChIP-PCR assay (Figure 4D). Simultaneously, dual-luciferase assay showed that overexpression of KLF9 enhanced luciferase activity in the PHLPP2-WT group of 293T cells (Figure 4E). Moreover, KLF9 overexpression led to increased PHLPP2 at mRNA and protein levels (Figures 4F, 4G). Of note, western blot exhibited that KLF9 overexpression elevated the level of KLF9 and inhibited the phosphorylation level of AKT (Figure 4F). Collectively, KLF9 enhanced PHLPP2 expression by interacting with the PHLPP2 promoter to inactivate the AKT pathway.

SLC7A11-AS1 promoted STUB1-mediated ubiquitination degradation of KLF9. Based on the above-mentioned results, we raised the question of whether KLF9 is involved in SLC7A11-AS1-mediated tumor progression. To address this question, firstly, SLC7A11-AS1 expression was silenced using sh-SLC7A11-AS1 transfection. When SLC7A11-AS1 was silenced, the mRNA expression of KLF9 had no influences (Supplementary Figure S3). However, the protein level of KLF9 was greatly elevated after silencing SLC7A11-

AS1 (Figure 5A). Further experiments determined that SLC7A11-AS1 depletion attenuated the ubiquitination of KLF9 (Figure 5B, Supplementary Figure S4). In addition, after CHX treatment, SLC7A11-AS1 silencing observably inhibited the decay of KLF9 protein (Supplementary Figure S5). Ubibroswer predicted that various ubiquitination enzymes including SMURF1, SKP2, BTRC, MDM2, SMURF2, BRCA1, STUB1, FBXW11, SYVN1, and TRAF2 might be involved in regulating ubiquitination of KLF9 (Supplementary Figure S2B). Co-IP assay validated that KLF9 could interact with SKP2, BTRC, and STUB1 in Huh7 cells, but we only observed that STUB1 precipitated by KLF9 antibody was decreased following SLC7A11-AS1 knockdown (Supplementary Figure S6). Figure 5C shows that SLC7A11-AS1 knockdown suppressed the interaction between KLF9 and STUB1 in Huh7 and MHCC97H cells. Of note, a previous study indicated that lncRNA as a scaffold could regulate STUB1-mediated ubiquitination [19]. As expected, catRAPID predicted that SLC7A11-AS1 had a potential combination with STUB1 and KLF9 (Supple-
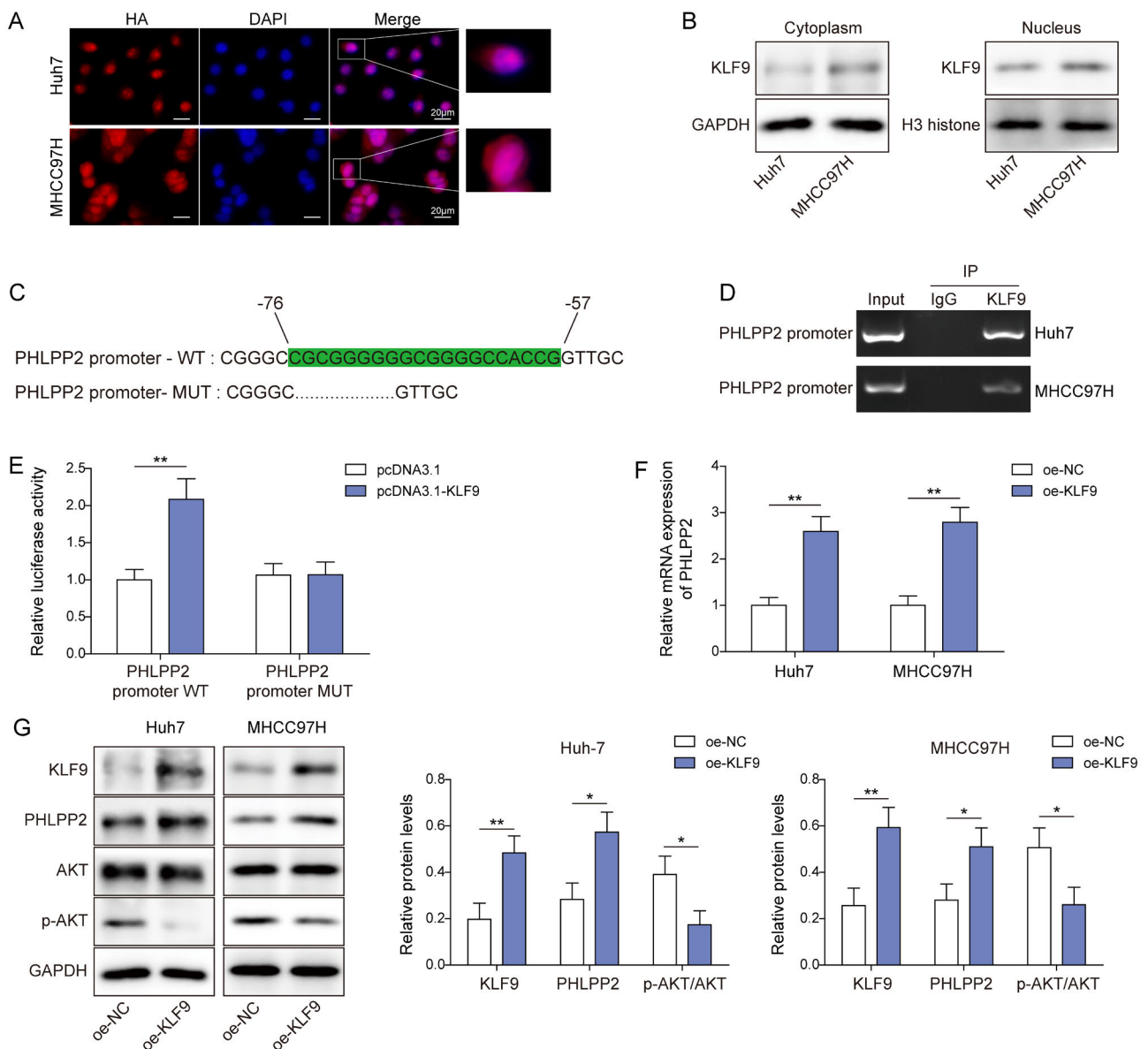
Figure 4. KLF9 activated PHLPP2 transcription to inhibit the AKT pathway. A) IF assay examined the location of KLF9 in Huh7 and MHCC97H cells. **B)** The location of KLF9 was detected using a nucleo-plasmic separation experiment. **C)** hTFtarget database predicated the binding sequences between KLF9 and PHLPP2 promoter. **D, E)** ChIP assay and dual luciferase assay verified the interaction between KLF9 and PHLPP2 promoter. Huh7 and MHCC97H cells were transfected with oe-KLF9 or oe-NC. **F)** RT-qPCR detected the expression of PHLPP2. **G)** Western blot evaluated protein levels of KLF9, PHLPP2, AKT, and p-AKT.

mentary Figures S2C, S2D). Furthermore, the IF-FISH assay revealed that SLC7A11-AS1 and KLF9 were co-located in the cytoplasm (Supplementary Figure S7A). Similarly, the co-location of SLC7A11-AS1 and STUB1 was validated in the cytoplasm (Supplementary Figure S7B). Further experiments found KLF9 and STUB1 also co-localized in the cytoplasm (Supplementary Figure S7C). Then, we separated the cytoplasm of Huh7 and MHCC97H cells. Co-IP revealed the combination between KLF9 and STUB1 in the cytoplasm (Supplementary Figure S7D). RIP assay revealed

KLF9 and STUB1 enriched SLC7A11-AS1 in Huh7 and MHCC97H cells (Figure 5D, Supplementary Figure S7E). In addition, SLC7A11-AS1 sense could pull down KLF9 and STUB1 in Huh7 and MHCC97H cells (Figure 5E). These results validated that SLC7A11-AS1 interacted with KLF9 and STUB1. Subsequently, oe-STUB1 was transfected into SLC7A11-AS1-silenced MHCC97H cells. SLC7A11-AS1 knockdown increased the KLF9 protein level and inhibited the ubiquitination of KLF9, while STUB1 overexpression decreased the KLF9 protein level and enhanced the ubiqui-
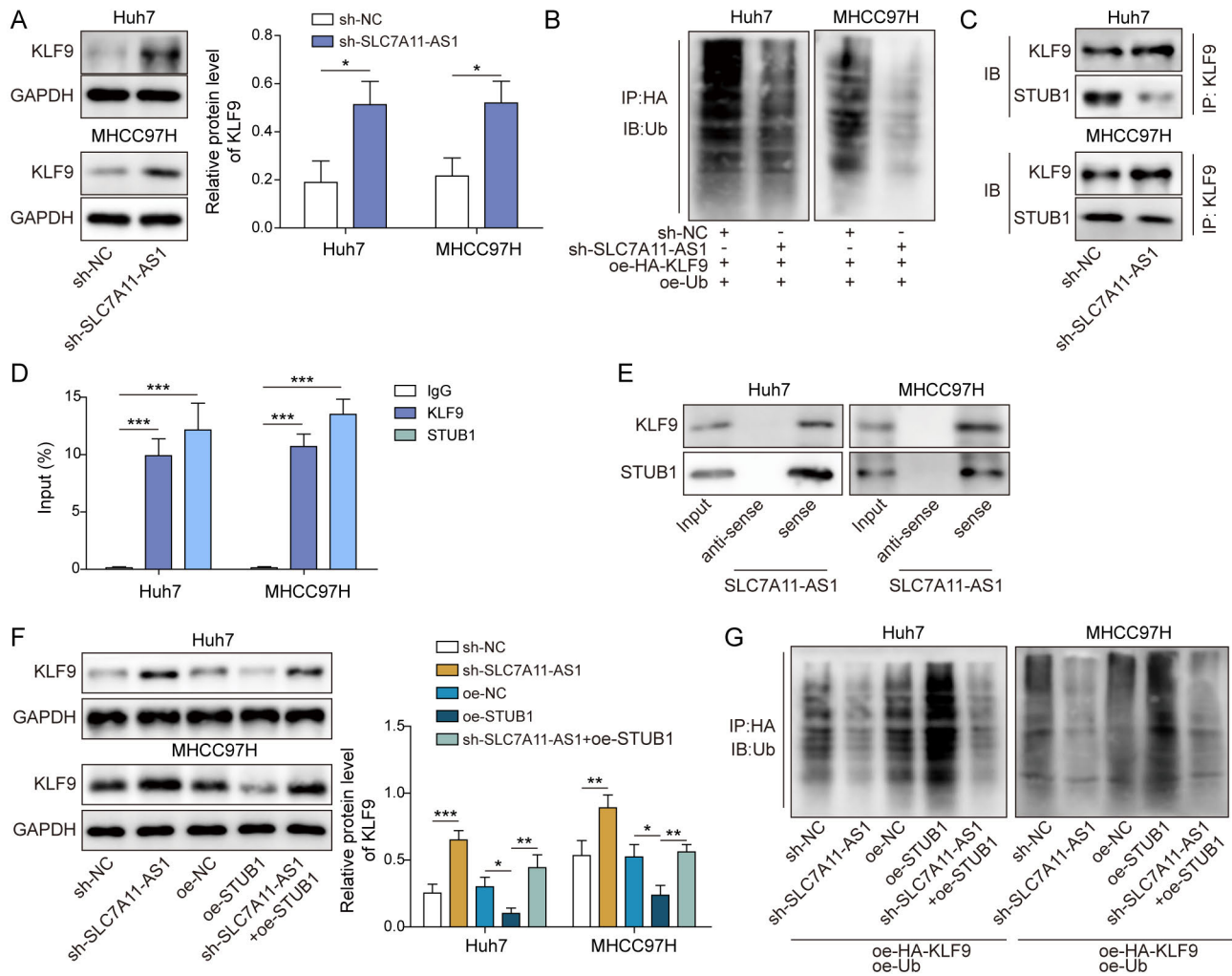
Figure 5. SLC7A11-AS1 promoted STUB1-mediated ubiquitination degradation of KLF9. A) Western blot evaluated the protein levels of KLF9 in sh-SLC7A11-AS1-transfected Huh7 and MHCC97H cells. **B)** Western blot detected KLF9 ubiquitination in sh-SLC7A11-AS1-transfected Huh7 and MHCC97H cells. **C)** Co-IP validated the interaction between KLF9 and STUB1. **D, E)** RIP and RNA pulldown verified the interaction of KLF9/SL-C7A11-AS1 and STUB1/SLC7A11-AS1 in Huh7 and MHCC97H cells. oe-STUB1 was transfected into SLC7A11-AS1-silenced MHCC97H cells. **F)** Western blot evaluated protein levels of KLF9. **G)** Western blot detected KLF9 ubiquitination.

tination of KLF9. Of note, sh-SLC7A11-AS1 in combination with oe-STUB1 transfection failed to reverse SLC7A11-AS1 knockdown-mediated promotion of KLF9 at the protein level and suppression of KLF9 ubiquitination (Figures 5F, 5G). Taken together, SLC7A11-AS1 played an important regulatory role in the STUB1-mediated ubiquitination degradation of KLF9.
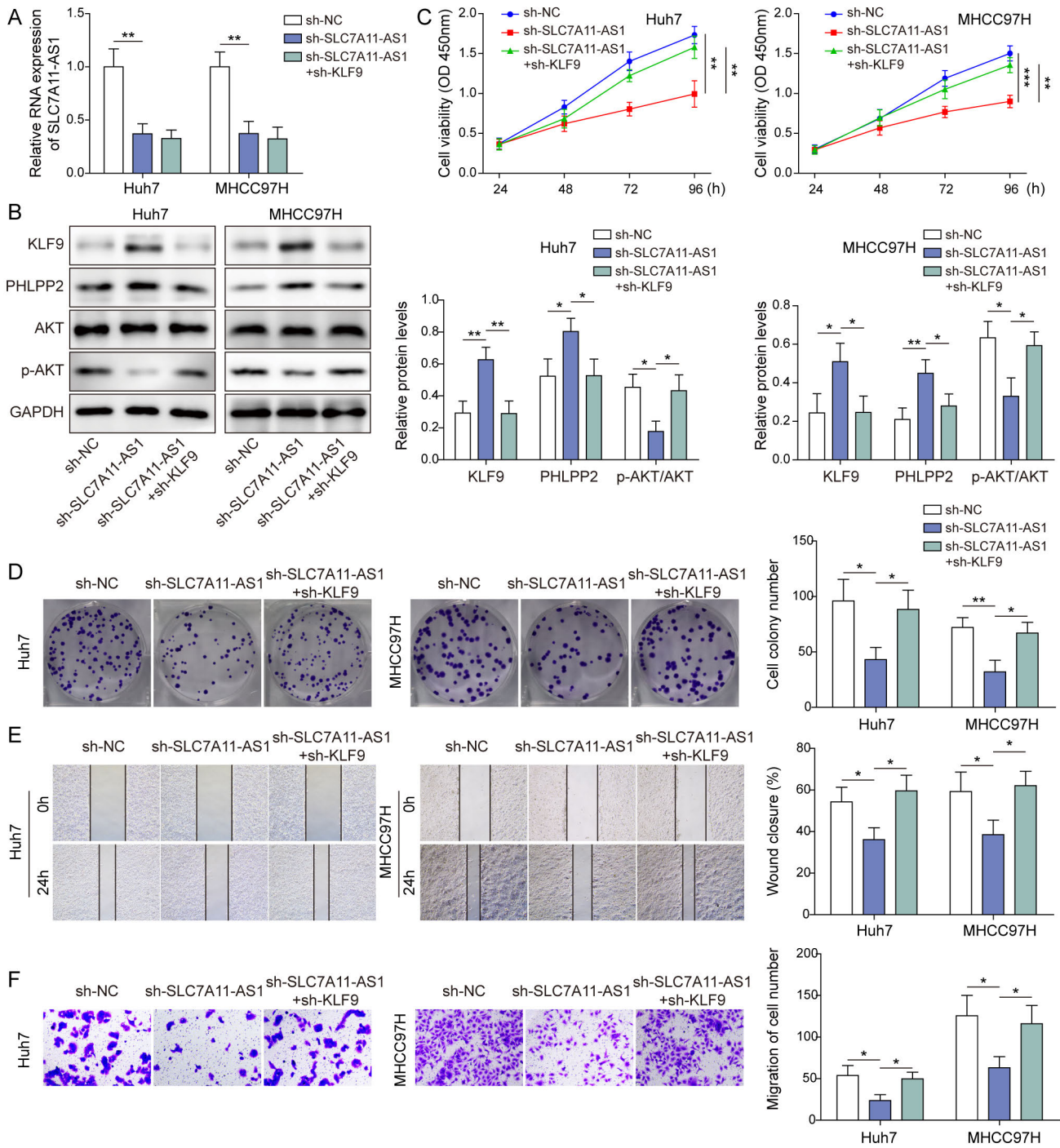
SLC7A11-AS1 accelerated cell viability, proliferation, migration, and invasion of HCC cells by decreasing the KLF9 expression. To investigate whether KLF9 is implicated in SLC7A11-AS1-mediated malignant behaviors of HCC cells, rescue experiments were conducted. sh-SLC7A11-AS1 with or without sh-KLF9 were transfected into Huh7 and MHCC97H cells. SLC7A11-AS1 expression was evidently declined by sh-SLC7A11-AS1 transfection, however, KLF9

knockdown failed to influence SLC7A11-AS1 expression (Figure 6A). SLC7A11-AS1 depletion apparently elevated KLF9 and PHLPP2 protein levels while decreasing the p-AKT protein level, whereas these alterations were abolished by KLF9 silencing (Figure 6B). SLC7A11-AS1 depletion-mediated suppressing influences on cell viability, proliferation, migration, and invasion were compromised by KLF9 silencing (Figures 6C–6F). To sum up, SLC7A11-AS1 suppression restrained malignant behaviors of HCC cells through elevating KLF9 expression.

SLC7A11-AS1 accelerated tumor growth and metastasis *in vivo* by decreasing the KLF9 expression. We established *in vivo* experiments to validate the results, which were obtained *in vitro*. MHCC97H cells were subjected to sh-SLC7A11-AS1 or in combination with sh-KLF9 trans-

fection. Western blot exhibited that the protein level of KLF9 was elevated by sh-SLC7A11-AS1, but sh-KLF9 transfection reversed the effect of sh-SLC7A11-AS1 on KLF9 protein level (Supplementary Figure S1B). The trans-

fected cells were injected subcutaneously into BALB/c nude mice. The tumors were removed from the mice 5 weeks after inoculation. SLC7A11-AS1 depletion notably diminished tumor size and weight, which were reversed by KLF9


Figure 6. SLC7A11-AS1 accelerated cell viability, proliferation, migration, and invasion of HCC cells by decreasing the KLF9 expression. sh-KLF9 was transfected into SLC7A11-AS1-silenced Huh7 and MHCC97H cells. A) RT-qPCR detected the expression of SLC7A11-AS1. B) Western blot evaluated protein levels of KLF9, PHLPP2, AKT, and p-AKT. C) CCK-8 assay detected cell viability. D) Clone formation examined cell proliferation. E) Wound-healing tested cell migration. F) Transwell determined cell invasion.

knockdown (Figures 7A–7C). SLC7A11-AS1 depletion-mediated suppression of Ki67 and elevation of KLF9 and PHLPP2 were attenuated by KLF9 knockdown (Figure 7D). In addition, MHCC97H cells with sh-SLC7A11-AS1 transfection or together with sh-KLF9 transfection were injected into nude mice through the tail vein to investigate the metastatic ability of HCC cells. We observed that KLF9 knockdown abrogated SLC7A11-AS1 depletion-mediated attenuation of metastasis ability to lungs (Figures 7E, 7F). These observations suggested that SLC7A11-AS1 depletion suppressed tumor growth and metastasis through increasing KLF9 expression.

Discussion

Due to its extremely high malignancy and rapid progression, HCC poses a serious threat to the life of patients. It has been reported that the 5-year survival rate of HCC patients after surgical resection of larger tumors was merely approximately 30% [28]. Therefore, seeking effective methods to improve the prognosis of HCC patients deserve to be explored. In this study, we found that SLC7A11-AS1 promoted tumor growth and metastasis of HCC *in vivo*. Moreover, *in vitro* experiments revealed that SLC7A11-AS1 accelerated cell viability, proliferation, migration, and
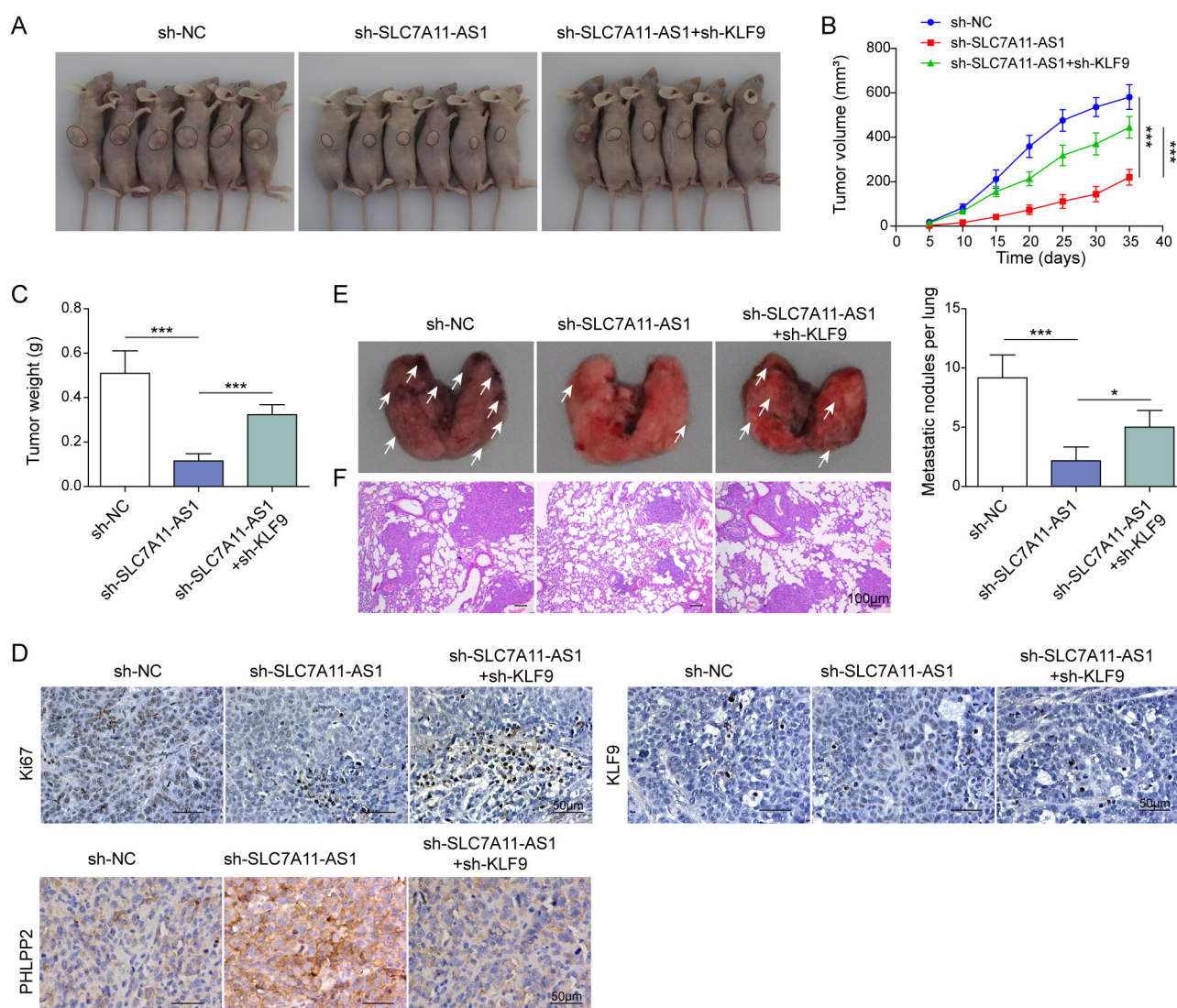
Figure 7. SLC7A11-AS1 accelerated tumor growth and metastasis *in vivo* through decreasing KLF9 expression. MHCC97H cells transfected with sh-SLC7A11-AS1 or in combination with sh-KLF9 were injected subcutaneously into BALB/c nude mice. A) The images of tumors in mice. B) Tumor sizes. C) Tumor weight. D) IHC detected Ki-67, KLF9, and PHLPP2 expression. MHCC97H cells transfected with sh-SLC7A11-AS1 or in combination with sh-KLF9 were injected into nude mice through the tail vein. E) The images of the lungs of nude mice. F) HE staining evaluated metastatic pulmonary nodules.

invasion of HCC by targeting the STUB1/KLF9/PHLPP2/AKT axis.

Growing evidences have confirmed that lncRNAs affected HCC progression by regulating the malignant characteristics of HCC [29]. For instance, lncRNA LIPCAR was enhanced observably in HCC cells and facilitated HCC cell growth and metastasis [30]. Lin *et al.* proposed that increased lncRNA COX7C-5 expression in HCC patients was positively related to unfavorable prognosis and lncRNA COX7C-5 knockdown notably suppressed malignant behaviors of HCC through regulating miR-581/ZEB2 axis [31]. SLC7A11-AS1 was identified to have abnormally high expression in multi-tumors including breast cancer, pancreatic cancer, and HCC [32–34]. On the whole, there are few studies on SLC7A11-AS1 in tumors, and the molecular mechanism of SLC7A11-AS1 and why it was highly expressed in various tumors are not clear. Here, the role of SLC7A11-AS1 in HCC and its upstream regulatory mechanism was focused on. Our findings revealed that SLC7A11-AS1 had abnormally high expression in five HCC cell lines including HepG2, Huh7, Bel-7405, Hep 3B2.1-7, and MHCC97H cells. SLC7A11-AS1 knockdown evidently suppressed cell viability, proliferation, migration, and invasion *in vitro* and inhibited tumor growth and metastasis *in vivo*. Furthermore, higher levels of m6A modification of SLC7A11-AS1 were observed in Huh7 and MHCC97H cells. m6A modification is the most common modification in mRNA and non-coding RNA relating to affect cancers [35, 36]. As previously reported, METTL3 was responsible for m6A modification of lncRNA ILF3-AS1 and enhanced lncRNA ILF3-AS1 expression, which promoted HCC progression [37]. In the current study, METTL3, a crucial methylase, mediated SLC7A11-AS1 m6A modification to elevate SLC7A11-AS1 expression in HCC, which might be one of the reasons for the high expression of SLC7A11-AS1 in HCC.

Transcription factor KLF9 has been widely explored in tumors. For instance, miRNA-494-3p decreased KLF9 expression to facilitate the progression of bladder cancer [38]; KLF9 regulated by TPTEP1/miR-548d-3p axis inhibited cell migration and invasion of gastric cancer [39]; miR-889-5p could downregulate KLF9 expression to accelerate HCC progression [40], which demonstrated that KLF9 had abnormally low expression and KLF9 overexpression generated the suppressing influence on the progression of tumors including HCC. Here, we explored the downstream target of KLF9. PHLPP2 is a phosphatase, and massive studies have found that the expression of PHLPP2 was decreased in multi-tumors, such as oral squamous cell carcinoma, lung cancer [41, 42]. A review suggested that PHLPP2 had a favorable prognosis for lung cancer, breast cancer, and colon cancer [43]. Moreover, a study published in 2018 proposed that berberine inhibited the AKT pathway to suppress HCC progression by enhancing PHLPP2 expression [23], suggesting PHLPP2 plays a suppressing role in HCC. Through bioinformatics analysis, ChIP-PCR, and dual-luciferase assay experiments, PHLPP2 was determined as a targeted gene of transcription factor KLF9 and positively regulated by KLF9. Notably, many studies have pointed out that PHLPP2 could mediate AKT dephosphorylation to inactivate the AKT activity in tumors including HCC and activation of the AKT pathway is positively correlated with tumor progression [22, 23, 44]. In this work, KLF9 overexpression elevated PHLPP2 expression and decreased p-AKT in Huh7 and MHCC97H cells. Taken together, the inhibition of HCC progression by KLF9 was achieved by mediating the PHLPP2/AKT axis.

Intriguingly, we found KLF9 mRNA expression was not changed while its protein level was increased in HCC cells when SLC7A11-AS1 was knockdown. As is well-known, ubiquitination refers to the process of linking ubiquitin molecules to protein substrates under a series of special enzymes including ubiquitin-activating enzyme E1, ubiquitin-binding enzyme E2, ubiquitin ligase E3, further degrading protein substrates [45]. Therefore, we thought SLC7A11-AS1 might regulate the protein level of KLF9 by ubiquitination of KLF9. Furthermore, SLC7A11-AS1 silencing suppressed the ubiquitination of KLF9 in HCC cells. Ubiquitin ligase E3 determines the specific recognition of target proteins and plays an important role in the ubiquitin pathway [46]. Previous studies have evidenced that lncRNAs could mediate the ubiquitination of proteins in the ubiquitin ligase E3-dependent manner, thus participating in regulating pathological conditions [47]. For instance, LINC00926 enhanced STUB1 (ubiquitin ligase E3)-mediated PGK1 ubiquitination to decrease PGK1 level in breast cancer [18]. LncRNA MTSS1-AS was reported to decrease MZF1 level by regulating STUB1-mediated MZF1 ubiquitination in pancreatic cancer [19]. In our study, we found that KLF9 was the substrate of STUB1 by Ubibrower predication and Co-IP experiments. SLC7A11-AS1 could interact with STUB1 and KLF9. However, we have not further explored the specific binding region among SLC7A11-AS1, STUB1, and KLF9, which will be the direction of our next research. Moreover, biological experiments exhibited that KLF9 knockdown could abolish sh-SLC7A11-AS1-mediated suppressing influences on cell viability, proliferation, migration and invasion of HCC cells, and tumor growth and metastasis of mice. Therefore, our findings revealed that SLC7A11-AS1 knockdown inhibited STUB1-mediated KLF9 ubiquitination, thereby restraining HCC progression.

Based on these results, we summarized that SLC7A11-AS1, regulated by m6A modification, promoted STUB1-mediated KLF9 ubiquitination degradation, which inhibited PHLPP2 transcription to activate AKT pathway, eventually accelerating HCC progression. Our findings might provide new therapeutic targets for HCC treatment.

Supplementary information is available in the online version of the paper.

References

[1] SUNG H, FERLAY J, SIEGEL RL, LAVERSANNE M, SO-ERJOMATARAM I et al. Global Cancer Statistics 2020: GLOBOCAN Estimates of Incidence and Mortality Worldwide for 36 Cancers in 185 Countries. CA Cancer J Clin 2021; 71: 209–249. https://doi.org/10.3322/caac.21660

[2] JUN L, YANG G, ZHISU L. The utility of serum exosomal microRNAs in hepatocellular carcinoma. Biomed Pharmacother 2019; 111: 1221–1227. https://doi.org/10.1016/j.biopha.2018.12.131

[3] VOGEL A, MEYER T., SAPISOCHIN G, SALEM R, SABOROWSKI A. Hepatocellular carcinoma. Lancet 2022; 400: 1345–1362. https://doi.org/10.1016/S0140-6736(22)01200-4

[4] DU D, LIU C, QIN M, ZHANG X, XI T et al. Metabolic dysregulation and emerging therapeutical targets for hepatocellular carcinoma. Acta Pharm Sin B, 2022. 12(2): p. 558–580. https://doi.org/10.1016/j.apsb.2021.09.019

[5] FARZANEH M, GHASEMIAN M, GHAEDRAHMATI F, POODINEH J, NAJAFI S et al. Functional roles of lncRNA-TUG1 in hepatocellular carcinoma. Life Sci 2022; 308: 120974. https://doi.org/10.1016/j.lfs.2022.120974

[6] WANG Y, TAN K, HU W, HOU Y, YANG G. LncRNA AC026401.3 interacts with OCT1 to intensify sorafenib and lenvatinib resistance by activating E2F2 signaling in hepatocellular carcinoma. Exp Cell Res 2022; 420: 113335. https://doi.org/10.1016/j.yexcr.2022.113335

[7] YANG Y, CHEN L, GU J, ZHANG H, YUAN J et al. Recurrently deregulated lncRNAs in hepatocellular carcinoma. Nat Commun 2017; 8: 14421. https://doi.org/10.1038/ncomms14421

[8] ZHANG L, WANG C, LU X, XU X, SHI T et al. Transcriptome sequencing of hepatocellular carcinoma uncovers multiple types of dysregulated ncRNAs. Front Oncol 2022; 12: 927524. https://doi.org/10.3389/fonc.2022.927524

[9] LI L, XIE R, LU G. Identification of m6A methyltransferase-related lncRNA signature for predicting immunotherapy and prognosis in patients with hepatocellular carcinoma. Biosci Rep 2021; 41: BSR20210760. https://doi.org/10.1042/BSR20210760

[10] ZHAO BS, ROUNDTREE IA, HE C. Post-transcriptional gene regulation by mRNA modifications. Nat Rev Mol Cell Biol 2017; 18: 31–42. https://doi.org/10.1038/nrm.2016.132

[11] FANG QY, DENG QF, LUO J, ZHOU CC. MiRNA-20a-5p accelerates the proliferation and invasion of non-small cell lung cancer by targeting and downregulating KLF9. Eur Rev Med Pharmacol Sci 2020; 24: 2548–2556. https://doi.org/10.26355/eurrev_202003_20522

[12] LI Y, SUN Q, JIANG M, LI S, ZHANG J et al. KLF9 suppresses gastric cancer cell invasion and metastasis through transcriptional inhibition of MMP28. FASEB J 2019; 33: 7915–7928. https://doi.org/10.1096/fj.201802531R

[13] SHAN L, SONG P, ZHAO Y, AN N, XIA Y et al. miR-600 promotes ovarian cancer cells stemness, proliferation and metastasis via targeting KLF9. J Ovarian Res 2022; 15: 52. https://doi.org/10.1186/s13048-022-00981-7

[14] SUN J, WANG B, LIU Y, ZHANG L, MA A et al. Transcription factor KLF9 suppresses the growth of hepatocellular carcinoma cells in vivo and positively regulates p53 expression. Cancer Lett 2014; 355: 25–33. https://doi.org/10.1016/j.canlet.2014.09.022

[15] SHAID S, BRANDTS CH, SERVE H, DIKIC I. Ubiquitination and selective autophagy. Cell Death Differ 2013; 20: 21–30. https://doi.org/10.1038/cdd.2012.72

[16] SEO J, LEE EW, SUNG H, SEONG D, DONDELINGER Y et al. CHIP controls necroptosis through ubiquitylation- and lysosome-dependent degradation of RIPK3. Nat Cell Biol 2016; 18: 291–302. https://doi.org/10.1038/ncb3314

[17] XIN H, XU X, LI L, NING H, RONG Y et al. CHIP controls the sensitivity of transforming growth factor-beta signaling by modulating the basal level of Smad3 through ubiquitin-mediated degradation. J Biol Chem 2005; 280: 20842–20850. https://doi.org/10.1074/jbc.M412275200

[18] CHU Z, HUO N, ZHU X, LIU H, CONG R et al. FOXO3A-induced LINC00926 suppresses breast tumor growth and metastasis through inhibition of PGK1-mediated Warburg effect. Mol Ther 2021; 29: 2737–2753. https://doi.org/10.1016/j.ymthe.2021.04.036

[19] HU Y, WANG F, XU F, FANG K, FANG Z et al. A reciprocal feedback of Myc and lncRNA MTSS1-AS contributes to extracellular acidity-promoted metastasis of pancreatic cancer. Theranostics 2020; 10: 10120–10140. https://doi.org/10.7150/thno.49147

[20] KANAN Y, MATSUMOTO H, SONG H, SOKOLOV M, ANDERSON RE et al. Serine/threonine kinase akt activation regulates the activity of retinal serine/threonine phosphatases, PHLPP and PHLPPL. J Neurochem 2010; 113: 477–488. https://doi.org/10.1111/j.1471-4159.2010.06609.x

[21] LIU N, JIANG X, GUO L, ZHANG C, JIANG M et al. Mutant p53 achieved Gain-of-Function by promoting tumor growth and immune escape through PHLPP2/AKT/PD-L1 pathway. Int J Biol Sci 2022; 18: 2419–2438. https://doi.org/10.7150/ijbs.67200

[22] SHI X, YANG J, LIU M, ZHANG Y, ZHOU Z et al. Circular RNA ANAPC7 Inhibits Tumor Growth and Muscle Wasting via PHLPP2-AKT-TGF-β Signaling Axis in Pancreatic Cancer. Gastroenterology 2022; 162: 2004–2017.e2. https://doi.org/10.1053/j.gastro.2022.02.017

[23] SAXENA S, SHUKLA S, KAKKAR P. Berberine induced modulation of PHLPP2-Akt-MST1 kinase signaling is coupled with mitochondrial impairment and hepatoma cell death. Toxicol Appl Pharmacol 2018; 347: 92–103. https://doi.org/10.1016/j.taap.2018.03.033

[24] ZHANG R, ZHANG G, LI B, WANG J, WANG J et al. Analysis of LINC01314 and miR-96 Expression in Colorectal Cancer Patients via Tissue Microarray-Based Fluorescence In Situ Hybridization. Dis Markers 2022; 2022: 5378963. https://doi.org/10.1155/2022/5378963

[25] LU Y, LIU X, XIE M, LIU M, YE M et al. The NF-κB-Responsive Long Noncoding RNA FIRRE Regulates Post-transcriptional Regulation of Inflammatory Gene Expression through Interacting with hnRNPU. J Immunol 2017; 199: 3571–3582. https://doi.org/10.4049/jimmunol.1700091

[26] ZENG X, HERNANDEZ-SANCHEZ W, XU M, WHITED TL, BAUS D et al. Administration of a Nucleoside Analog Promotes Cancer Cell Death in a Telomerase-Dependent Manner. Cell Rep 2018; 23: 3031–3041. https://doi.org/10.1016/j.celrep.2018.05.020

[27] ZHANG H, LIU Y, WANG W, LIU F, WANG W et al. ALKBH5-mediated m(6)A modification of lincRNA LINC02551 enhances the stability of DDX24 to promote hepatocellular carcinoma growth and metastasis. Cell Death Dis 2022; 13: 926. https://doi.org/10.1038/s41419-022-05386-4

[28] GALLE PR, TOVOLI F, FOERSTER F, WÖRNS MA, CUCCHETTI A et al. The treatment of intermediate stage tumours beyond TACE: From surgery to systemic therapy. J Hepatol. 2017; 67: 173–183. https://doi.org/10.1016/j.jhep.2017.03.007

[29] HAN TS, HUR K, CHO HS, BAN HS. Epigenetic Associations between lncRNA/circRNA and miRNA in Hepatocellular Carcinoma. Cancers (Basel) 2020; 12: 2622. https://doi.org/10.3390/cancers12092622

[30] BONGOLO CC, THOKERUNGA E, FIDELE NB, SOURAKA TDM et al. Upregulation of the long non-coding RNA, LIPCAR promotes proliferation, migration, and metastasis of hepatocellular carcinoma. Cancer Biomark 2022; 35: 245–256. https://doi.org/10.3233/CBM-220033

[31] LIN Y, WANG F, ZHONG Y, CHENG NM, XIONG J et al. Long non-coding RNA COX7C-5 promotes hepatocellular carcinoma progression via miR-581/ZEB2 axis. Cell Signal 2023; 101: 110501. https://doi.org/10.1016/j.cellsig.2022.110501

[32] LIANG J, LIAO J, LIU T, WANG Y, WEN J et al. Comprehensive analysis of TGF-β-induced mRNAs and ncRNAs in hepatocellular carcinoma. Aging (Albany NY) 2020; 12: 19399–19420. https://doi.org/10.18632/aging.103826

[33] SYNNOTT NC, MADDEN SF, BYKOV VJN, CROWN J, WIMAN KG et al. The Mutant p53-Targeting Compound APR-246 Induces ROS-Modulating Genes in Breast Cancer Cells. Transl Oncol 2018; 11: 1343–1349. https://doi.org/10.1016/j.tranon.2018.08.009

[34] YANG Q, LI K, HUANG X, ZHAO C, MEI Y et al. lncRNA SLC7A11-AS1 Promotes Chemoresistance by Blocking SCF(β-TRCP)-Mediated Degradation of NRF2 in Pancreatic Cancer. Mol Ther Nucleic Acids 2020; 19: 974–985. https://doi.org/10.1016/j.omtn.2019.11.035

[35] HE Y, DU X, CHEN M, HAN L, SUN J et al. Novel insight into the functions of N6-methyladenosine modified lncRNAs in cancers (Review). Int J Oncol 2022; 61: 152. https://doi.org/10.3892/ijo.2022.5442

[36] PETRI BJ, KLINGE CM. m6A readers, writers, erasers, and the m6A epitranscriptome in breast cancer. J Mol Endocrinol 2022; 70: e220110. https://doi.org/10.1530/JME-22-0110

[37] BO C, LI N, HE L, ZHANG S, AN Y. Long non-coding RNA ILF3-AS1 facilitates hepatocellular carcinoma progression by stabilizing ILF3 mRNA in an m(6)A-dependent manner. Hum Cell 2021; 34: 1843–1854. https://doi.org/10.1007/s13577-021-00608-x

[38] XU XH, SUN JM, CHEN XF, ZENG XY, ZHOU HZ et al. MicroRNA-494-3p facilitates the progression of bladder cancer by mediating the KLF9/RGS2 axis. Kaohsiung J Med Sci 2022; 38: 1070–1079. https://doi.org/10.1002/kjm2.12588

[39] HUANG Y, WANG J, ZHANG H, XIANG Y, DAI Z et al. LncRNA TPTEP1 inhibits the migration and invasion of gastric cancer cells through miR-548d-3p/KLF9/PER1 axis. Pathol Res Pract 2022; 237: 154054. https://doi.org/10.1016/j.prp.2022.154054

[40] TANG Y, LI K, HU B, CAI Z, LI J et al. Fatty acid binding protein 5 promotes the proliferation, migration, and invasion of hepatocellular carcinoma cells by degradation of Krüppel-like factor 9 mediated by miR-889-5p via cAMP-response element binding protein. Cancer Biol Ther 2022; 23: 424–438. https://doi.org/10.1080/15384047.2022.2094670

[41] HUANG H, PAN X, JIN H, LI Y, ZHANG L et al. PHLPP2 Downregulation Contributes to Lung Carcinogenesis Following B[a]P/B[a]PDE Exposure. Clin Cancer Res 2015; 21: 3783–3793. https://doi.org/10.1158/1078-0432.CCR-14-2829

[42] LIU L, GUO B, HAN Y, XU S, LIU S. MARCH1 silencing suppresses growth of oral squamous cell carcinoma through regulation of PHLPP2. Clin Transl Oncol 2022; 24: 1311–1321. https://doi.org/10.1007/s12094-021-02769-5

[43] CHEN B, WANG T, ZHANG J, ZHANG S, SHANG X et al. Identification of Colon Cancer-Related RNAs Based on Heterogeneous Networks and Random Walk. Biology (Basel) 2022; 11: 1003. https://doi.org/10.3390/biology11071003

[44] TANTAI J, PAN X, CHEN Y, SHEN Y, JI C et al. TRIM46 activates AKT/HK2 signaling by modifying PHLPP2 ubiquitylation to promote glycolysis and chemoresistance of lung cancer cells. Cell Death Dis 2022; 13: 285. https://doi.org/10.1038/s41419-022-04727-7

[45] POPOVIC D, VUCIC D, DIKIC I. Ubiquitination in disease pathogenesis and treatment. Nat Med 2014; 20: 1242–1253. https://doi.org/10.1038/nm.3739

[46] TOMA-FUKAI S, SHIMIZU T. Structural Diversity of Ubiquitin E3 Ligase. Molecules 2021; 26: 6682. https://doi.org/10.3390/molecules26216682

[47] WANG LQ, ZHENG YY, ZHOU HJ, ZHANG XX, WU P et al. LncRNA-Fendrr protects against the ubiquitination and degradation of NLRC4 protein through HERC2 to regulate the pyroptosis of microglia. Mol Med 2021; 27: 39. https://doi.org/10.1186/s10020-021-00299-y

LncRNA SLC7A11-AS1 promotes the progression of hepatocellular carcinoma by mediating KLF9 ubiquitination

Fan-Lin ZENG[1,2], Jie LIN[3], Xing XIE[2], Yuan-Kang XIE[2], Jian-Hong ZHANG[2], Daofeng XU[2], Xiao HE[2], Feng En LIU[4], Bin-Hui XIE[2,*]
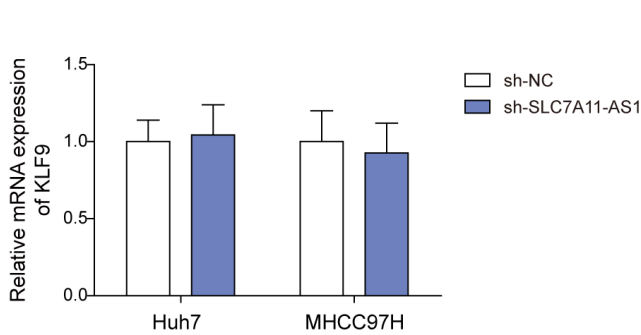
Supplementary Information
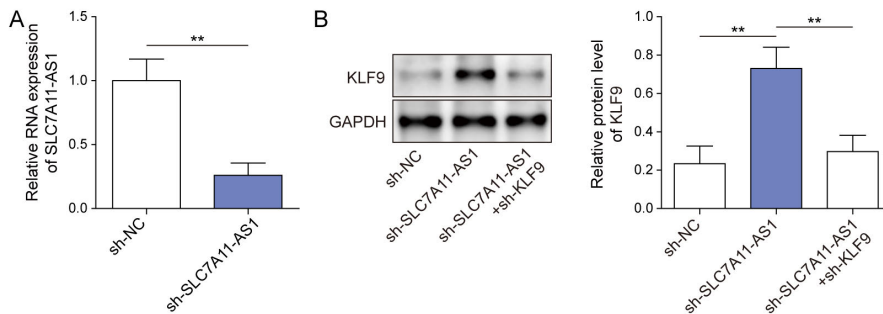
Supplementary Figure S1. The expression of SLC7A11-AS1 and KLF9. A) RT-qPCR detected the expression of SLC7A11-AS1 in MHCC97H cells transfected with sh-SLC7A11-AS1 or sh-NC. B) Western blot detected KLF9 level in MHCC97H cells transfected with sh-SLC7A11-AS1 or in combination with sh-KLF9.
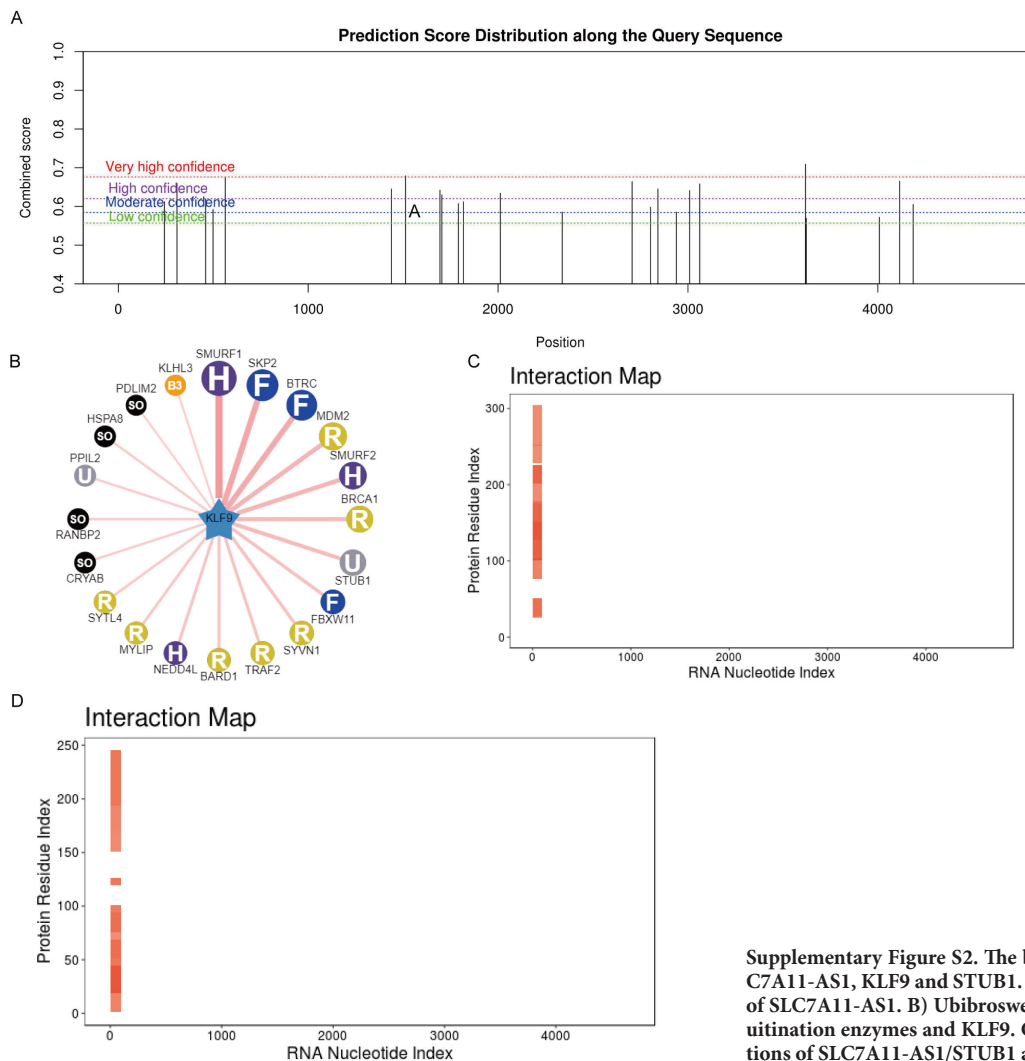

Supplementary Figure S2. The binding sites among METTL3, SLC7A11-AS1, KLF9 and STUB1. A) SRAMP predicted the m6A site of SLC7A11-AS1. B) Ubibroswer predicted between various ubiquitination enzymes and KLF9. C, D) catRAPID predicted interactions of SLC7A11-AS1/STUB1 and SLC7A11-AS1/KLF9.

Supplementary Figure S3. The mRNA expression of KLF9. RT-qPCR examined the expression of KLF9 in MHCC97H cells transfected with sh-SLC7A11-AS1 or sh-NC.
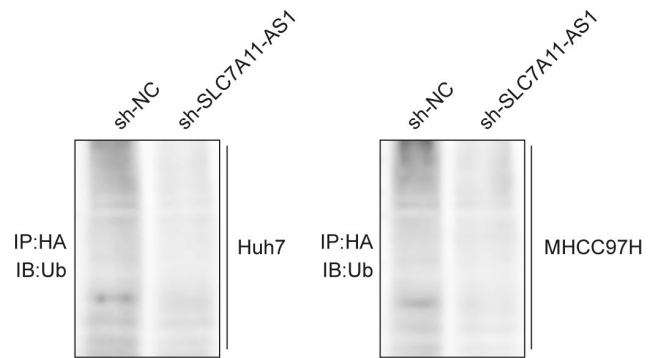
Supplementary Figure S4. The effect of KLF9 ubiquitination in sh-SLC7A11-AS1-transfected Huh7 and MHCC97H cells. Western blot detected KLF9 ubiquitination in sh-SLC7A11-AS1-transfected Huh7 and MHCC97H cells.
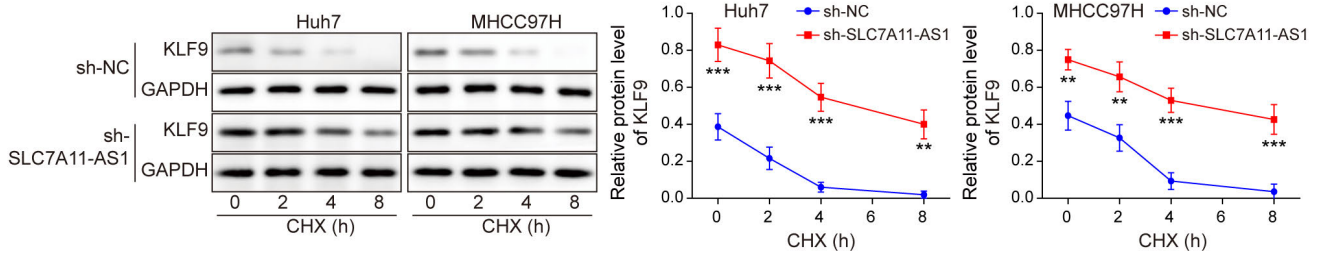
Supplementary Figure S5. SLC7A11-AS1 silencing affected the decay of KLF9 protein. Western blot detected KLF9 protein in Huh7 and MHCC97H cells after CHX treatment for 0, 2, 4 and 8 h.
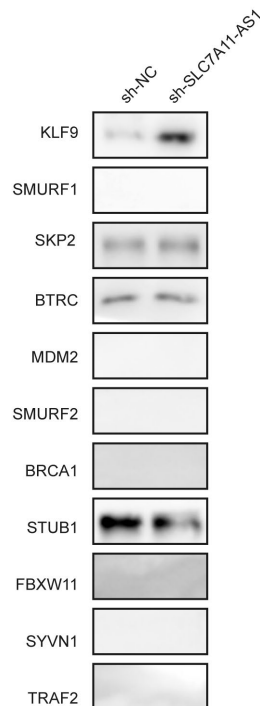
Supplementary Figure S6. The interactions of various ubiquitination enzymes and KLF9. Co-IP assay verified the interactions of various ubiquitination enzymes and KLF9.
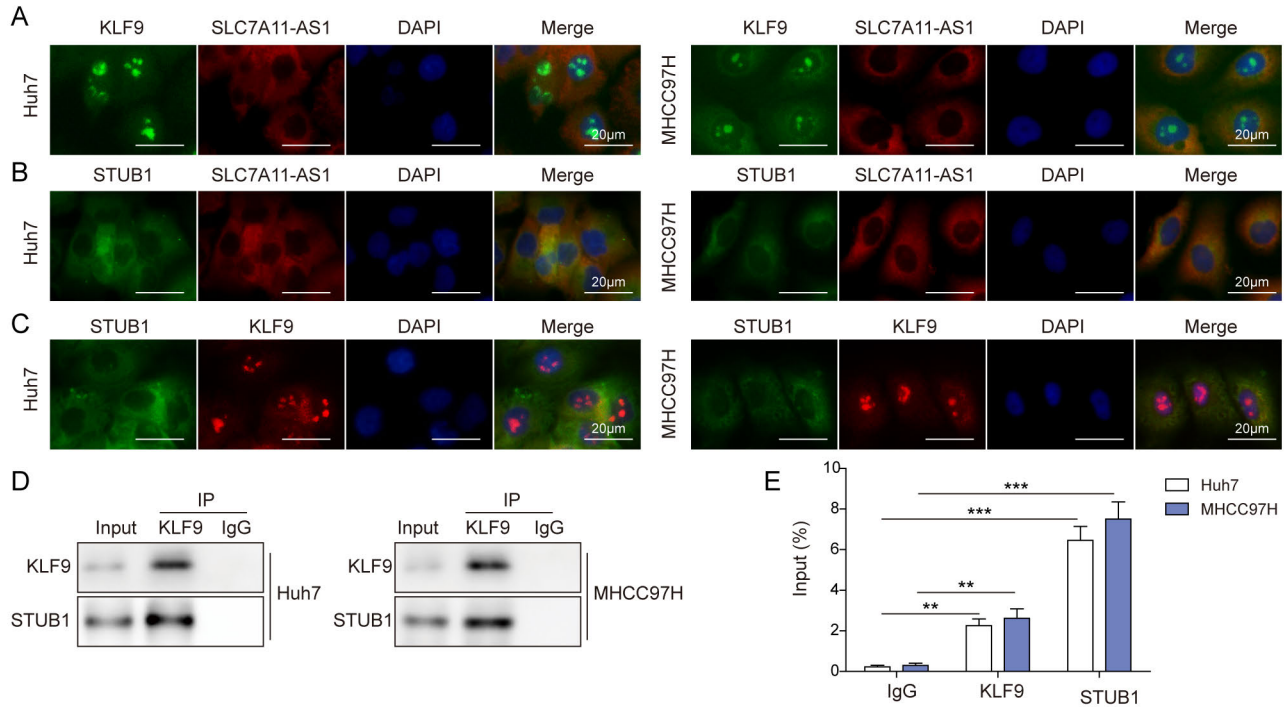
Supplementary Figure S7. The binding relationship of SLC7A11-AS1, KLF9 and STUB1 in cytoplasm of Huh7 and MHCC97H cells. A, B) IF-FISH assay was used to detect co-location of SLC7A11-AS1 and KLF9/STUB1 in Huh7 and MHCC97H cells. Red indicated the location of SLC7A11-AS1 and green indicated the location of KLF9 or STUB1. C) IF assay was applied to examine co-location of KLF9 and STUB1 in Huh7 and MHCC97H cells. D) Co-IP was used to validate the interaction between KLF9 and STUB1. E) RIP was used to validate the interaction between SLC7A11-AS1 and KLF9/STUB1.